Electrochromic Linear and Star Branched Poly(3,4-ethylenedioxythiophene−didodecyloxybenzene) Polymers

Fei Wang,* Michael S. Wilson, and R. David Rauh

EIC Laboratories, Inc., 111 Downey Street, Norwood, Massachusetts 02062

Philippe Schottland, Barry C. Thompson, and John R. Reynolds

Department of Chemistry, Center for Macromolecular Science and Engineering, University of Florida, Gainesville, Florida 32611

Received November 2, 1999; Revised Manuscript Received January 24, 2000

ABSTRACT: New linear and star structured poly(3,4-ethylenedioxythiophene−didodecyloxybenzenes) (PEBs) have been prepared which exhibit thermochromism and multicolor electrochromism as they are able to produce the three basic colors in the RGB system: red, green, and blue. The star polymer features a conjugated hyperbranched poly(triphenylamine) core with PEB arms ca. 8−10 repeat units (16−20 rings) in length. Red in solution, the optical spectra of both polymers exhibit a maximum absorption at 455 nm in the neutral state. Linear and star PEB are thermally stable up to 300 °C as demonstrated by TGA. The presence of an EDOT-phenylene repeat in the conjugated backbone results in a relatively low half-wave potential of +0.20 V vs Fc/Fc^+, which is lower than regioregular poly(3-hexylthiophene) by 0.4 V and only slightly higher than PEDOT. As a result, star PEB is the first representative of a new class of star-shaped polymers where it is possible to address the electroactive arms independently from the conjugated core. The redox switching properties of these star PEBs are quite stable with a 90% retention of electroactivity after 4500 double potential switches. These properties are of particular importance for electrochemically based display applications where highly stable processable electrochromic polymers are needed.

Introduction

Since the discovery of conductivity in conjugated polymers, the field of electronically conductive polymers has focused on linear conjugated systems which include polyacetylene, polypyrrole, polyaniline, polythiophene, and similar derivatives.[1] 3,4-Ethylenedioxythiophene (EDOT) is a commercially available monomer, and poly(3,4-ethylenedioxythiophene) (PEDOT) is a relatively new member in the conducting polymer family. PEDOT displays many interesting properties including low half-wave potential and band gap.[2] In addition, this polymer exhibits outstanding electrochemical stability upon cycling, as well as air and thermal stability of its electrical properties compared to other polythiophenes.[3] The ability of PEDOT to switch between a deep blue neutral state and a highly transmissive sky blue doped state makes this polymer a very interesting candidate for electrochromics.[4] Moreover, PEDOT and its derivatives have demonstrated fast switching with a high contrast ratio over a long period of time in single or dual electrochromic devices.[5−7]

Star polymers are usually defined as branched macromolecules that consist of linear polymer arms joined together by a central core.[8] To investigate the effect of conducting polymer structure on solid state properties, work was initiated by studying an electrically conducting polymer with a star structure[9] that contained an electroinactive hyperbranched poly(1,3,5-phenylene) core bearing regioregular poly(3-hexylthiophene) (P3HT) conducting arms. The results showed that, despite the branched structure, this star polymer was able to self-assemble into thin films with morphological, electrical, and optical properties that revealed a surprisingly high degree of structural order. More recently, we reported on a new conducting star polymer using a combination of a hyperbranched poly(triphenylamine) core and conjugated arms that, after doping, yield a fully conducting star structure.[10] In this instance, since the core is electroactive, charge carriers can be generated through the entire material, thus leading to a truly three-dimensional conductor. Characterization of the redox properties of this conducting star polymer was complicated by the similarity in the oxidation potential of both the core and the arms.

In this paper, we report the synthesis and characterization of the first example of an electroactive and conducting star polymer system where the redox activity of the core and the arms can be addressed independently. Using the same hyperbranched poly(triphenylamine) (PTPA) core introduced earlier, low oxidation potential electron-rich poly(3,4-ethylenedioxythiophene−didodecyloxybenzene) (PEB) arms were employed. In this work, both linear and star structured PEBs have been synthesized and are compared.

Results and Discussion

Synthesis. To overcome the difficulty of monofunctionalizing bis-EDOT-arylene units,[11] we have taken an approach to building the polymer from an EDOT-arylene monomer. This approach has two potential advantages. First, the EDOT-arylene unit is unsymmetric with controlled reactivity providing for a regioregular polymerization. Second, the ratio of EDOT to arylene is 1:1, providing a higher solubility than that observed for poly(bis-EDOT-arylene) due to the increased content of the long dialkoxy side chains.

The synthesis was carried out as outlined in Scheme 1 where a Stille coupling was employed to couple EDOT with1,4-dibromo-2,5-didodecyloxybenzene. Compound **2** was successfully brominated using NBS to give the

10.1021/ma9918506 CCC: $19.00
Published on Web 03/02/2000

Scheme 1

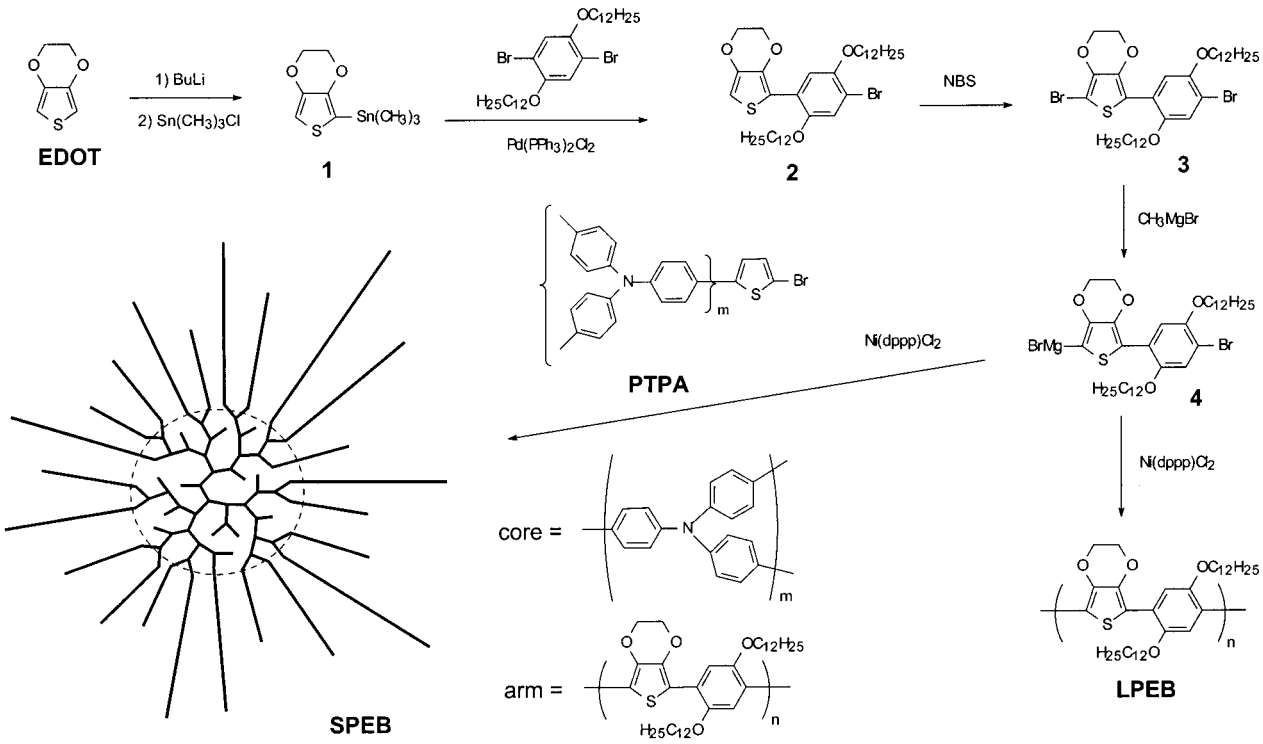

dibromo compound **3**. Following a procedure reported recently by McCullough et al.[12] for the preparation of regioregular poly(3-dodecylthiophene), the dibromo compound **3** was reacted with methylmagnesium bromide at reflux, followed by Ni(dppp)Cl_2-catalyzed polymerization of the bromomagnesio intermediate **4**. This led to the formation of a bright red linear polymer LPEB. The polymer was purified by Soxhlet extraction with hexane and methanol, to remove low molecular weight fractions and impurities.

A similar procedure was used to synthesize the star structured polymer SPEB. A solution of **4** was added dropwise to a solution containing bromothiophene-capped poly(triphenylamine) (PTPA) and Ni(dppp)Cl_2 catalyst. After reflux overnight and isolation, followed by purification by Soxhlet extraction with methanol and hexane, a bright red star polymer SPEB was obtained. As low molecular weight LPEB was soluble in hexane, during the Soxhlet extraction process, a significant amount of material was removed from LPEB, causing the yield of LPEB to be much lower than that of SPEB. In the star polymer synthesis, the Grignard reagent **4** is slowly added to the bromothiophene-capped PTPA. As this is a fast reaction as noticed by McCullough,[12] reaction preferentially occurs on the core, and long linear PEB chains not attached to the core do not form. Short PEB chains that are not attached to the core are removed by Soxhlet extraction with hexane, providing a relatively pure material.

Both LPEB and SPEB have a solubility of about 50 mg/mL in solvents including THF, chloroform, dichloromethane, and carbon disulfide. This solubility is enhanced relative to poly(bis-EDOT-arylene) polymers which are only slightly soluble in common organic solvents. Changing the ratio of EDOT to arylene from 2:1 to 1:1 has improved the solubility of the polymer.

Structural Characterization. In the results reported by McCullough,[12] the reaction of methylmagnesium bromide with 2,5-dibromo-3-docecylthiophene afforded the 5-bromomagnesio isomer in 80% and the 2-bromomagnesio isomer in 20% yields, respectively. In our case, there is a more distinct disparity in the reactivities to metalation due to the thienyl and phenyl sites on compound **3**. To confirm which aryl bromide is metalated more easily, **3** was reacted with methylmagnesium bromide and the intermediate quenched with water. The product had an ^{1}H NMR spectrum identical to that of compound **2**, featuring a $\delta = 6.4$ ppm proton signal from thiophene. Subsequently, the bromo-EDOT preferentially metalates, and polymerization proceeds to yield a very regular polymer.

The ^{1}H NMR of LPEB is consistent with polymerization as outlined in Scheme 1. The two phenylene protons observed for the monomer (7.09 and 7.67 ppm) are converted to a single peak at 7.67 ppm in the polymer due to the symmetrical repeat unit. The same effect is seen in the ^{1}H NMR of SPEB where a peak at 7.65 ppm integrating for the two phenylene protons is observed. In addition, a broad peak is observed between 7.3 and 7.8 ppm that corresponds with the PTPA core. The ^{1}H NMR integration result for SPEB has the expected aromatic to $-OCH_2-$ ratio, in agreement with the SEC characterization results.

Table 1. SEC Results for Polymers LPEB and SPEB

	M_w	M_w/M_n	$[\eta]$ (dL/g)
PTPA	6 800	1.56	0.049
LPEB	40 400	1.30	0.20
SPEB	65 700	2.05	0.25

SEC Characterization. The molecular weights of the polymers were approximated by size exclusion chromatography (SEC) equipped with an on-line light-scattering detector, viscometer, and refractive index detector and are summarized in Table 1. As explained earlier, the low molecular weight fraction of LPEB was removed by hexane extraction. The remaining LPEB exhibits a relatively high M_w of ca. 40 000 g mol^{-1} along with a narrow polydispersity index. While it is under-

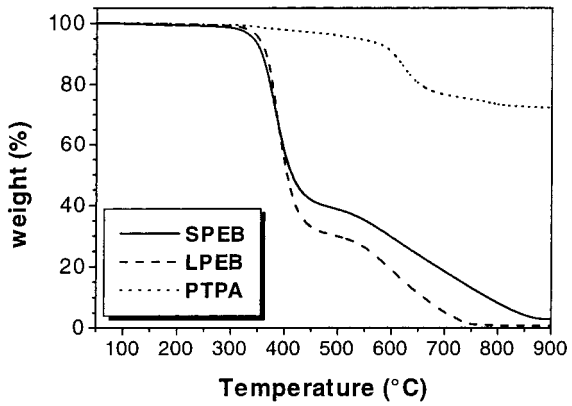

Figure 1. TGA thermograms of LPEB (dash), SPEB (solid), and PTPA (dotted) under nitrogen at a scan rate of 20 °C/min.

stood that these SEC results are approximate, the LPEB has on the order of 70 repeat units per polymer chain. As detailed in our previous report,[10] the star polymers synthesized using the PTPA core have an estimated number of 10−15 arms each. To avoid the formation of long linear PEB chains, we used a ratio of 10 monomer units per active site (ca. 100 monomers per star core) to ensure each arm is attached. Note that, due to the random nature of the coupling reaction in the star polymer synthesis, the lengths of the arms in the star is polydisperse, as depicted in Scheme 1. Using the SEC determined molecular weight differences between the final star polymer and the starting core, an approximate average degree of polymerization of 8 (16 rings) was determined for the SPEB arms. The intrinsic viscosity results obtained from the on-line detector further confirmed star formation in SPEB. It has been demonstrated for linear and star polybutadienes that the slopes of the lines in the Mark−Houwink plot are the same for linear and star polymers. This is also observed when comparing LPEB with SPEB. Similar Mark−Houwink exponents are observed for SPEB (0.64) and LPEB (0.68). However, the intercepts of these lines decrease with an increase in the number of arms in the star.[13] SPEB is found to have a smaller intercept than LPEB, as expected for the star polymer having a more highly branched and compact structure. The intrinsic viscosity values for SPEB and LPEB are in a similar range as observed for P3HT polymers.[10]

Thermal Properties. The thermal stability of these polymers was characterized by thermogravimetric analysis (TGA) under nitrogen. As illustrated by the TGA thermograms presented in Figure 1, both the star and linear PEBs are quite thermally stable up to 300 °C. This observation is in accordance with our previous results on star P3HT.[10] Both LPEB and SPEB begin to lose weight at temperatures above 350 °C with a first-stage weight loss of about 70% for LPEB and 60% for SPEB, likely due to cleavage of the dodecyloxy and ethylenedioxy side chains. As expected, the weight loss is less in SPEB because of the presence of the PTPA core which does not show a decomposition before 550 °C (also illustrated in Figure 1).

UV−vis Spectra. The solution UV−vis spectra for SPEB and LPEB are shown in Figure 2. The λ_{max} for the π to π^* transition is found at 455 nm in both polymers as the average length of the arms (20−30 EDOT-didodecyloxybenzene average rings) is sufficient to reach the polymer limit. Previously we showed that the PTPA core polymer has an absorbance at about 380 nm in solution,[10] and this is observable in SPEB as a slight absorbance increase. Because of the compositional dominance of the PEB arms in the star, the SPEB spectrum is dominated by the PEB absorption.

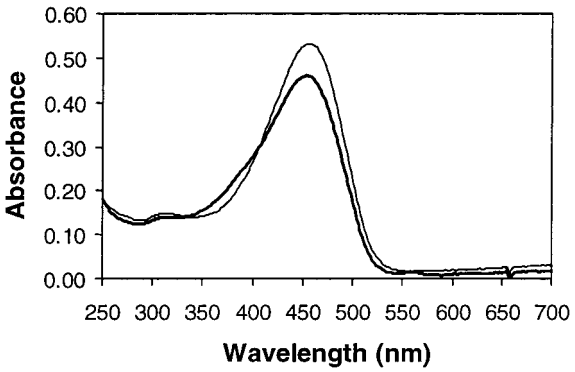

Figure 2. Solution UV−vis spectra of SPEB (bold) and LPEB (regular) in chloroform.

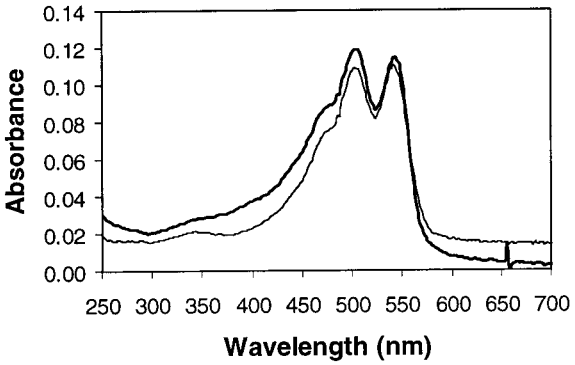

Figure 3. Solid-state UV−vis spectra of SPEB (bold) and LPEB (regular) from cast films on a quartz substrate.

The solid-state UV−vis spectra for both SPEB and LPEB are shown in Figure 3. As expected and is common in many conjugated polymers, the absorbance shifts to somewhat lower energies due to a more extended structure with fewer conformational defects. Interestingly, the π to π^* transition band has split into two peaks with λ_{max} at 502 and 542 nm. Similarly, a slightly higher absorbance exists in the SPEB spectrum at about 380 nm due to the PTPA core.

Thermochromism. Some polythiophenes bearing relatively long alkyl or alkoxy side chains are known to exhibit thermochromism, both in solid state and in solution.[14−18] Due to the presence of the two didodecyloxy chains on the benzene ring in the PEBs, the thermochromic properties of both LPEB and SPEB were investigated in the solid state. A strong thermochromic phenomenon was observed above 200 °C as both polymers changed from a bright red absorptive form to highly transmissive yellow. Above 240 °C no further significant change in the color of the polymer films was noticed. This blue shift is commonly attributed to planar to nonplanar conformational changes of the conjugated backbone.[16] The long side chains induce mobility upon heating which causes a twisting of the conjugated backbone. Therefore, the mean conjugation length decreases, leading to the blue shift.

Electrochemical Properties. The cyclic voltammograms of LPEB and SPEB are shown in Figures 4 and 5. As expected with EDOT-containing polymers, the half-wave potential of LPEB ($E_{1/2}$ = +0.20 V vs Fc/Fc^+) is lower than that of a regioregular poly(3-hexylth-

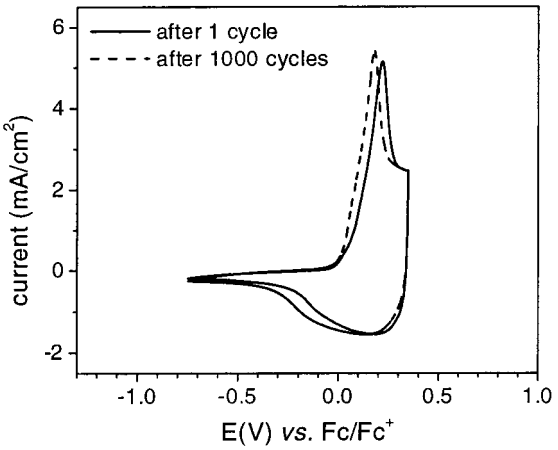

Figure 4. Cyclic voltammogram of LPEB as a function of repeated scans at 20 mV/s in 0.1 M $LiClO_4$/acetonitrile: after 1 cycle (plain), after 1000 cycles (dash).

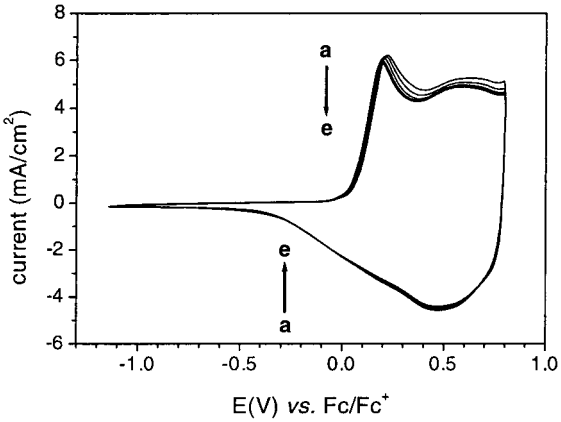

Figure 5. Cyclic voltammogram of SPEB in 0.1 M $LiClO_4$/acetonitrile as a function of repeated scans at 20 mV/s in 0.1 M $LiClO_4$/acetonitrile: (a) scan 2, (b) scan 5, (c) scan 10, (d) scan 15 and (e) scan 20.

iophene) ($E_{1/2}$ = +0.6 V vs Fc/Fc^+).[19] The cyclic voltammogram of LPEB between −0.75 and +0.35 V vs Fc/Fc^+ shows no decrease of the peak intensity after 1000 cycles, thus illustrating the outstanding stability of the redox process in this linear polymer. The electrochemical behavior of SPEB between −1.15 and +0.80 V vs Fc/Fc^+ (presented in Figure 5) features two oxidation peaks and a broad reduction. Comparable behavior has already been reported in our previous work on the similar poly(3-hexylthiophene) star polymer.[10] The origin of the oxidation peaks is fairly straightforward in this case, because the arms of the star polymer have a much lower oxidation potential than the electroactive core. Consequently, the first oxidation peak (E_{ox1} = +0.22 V vs Fc/Fc^+) corresponds to the PEB arms, while the second oxidation peak (E_{ox2} = +0.63 V vs Fc/Fc^+) is the response due to the PTPA core. Note that the oxidation potential of the PEB arms in the star polymer is almost the same as that of the linear PEB. To compare the stability of SPEB and LPEB upon cycling, SPEB was cycled in the same potential range as LPEB (−0.75 to +0.35 V vs Fc/Fc^+). In these conditions, and due to the oxidation peak separation, it is possible to address the arms independently of the core. A decrease of the anodic peak intensity of only 12% was observed after 500 cycles, thus emphasizing the excellent electrochemical stability of the PEB arms in the star polymer.

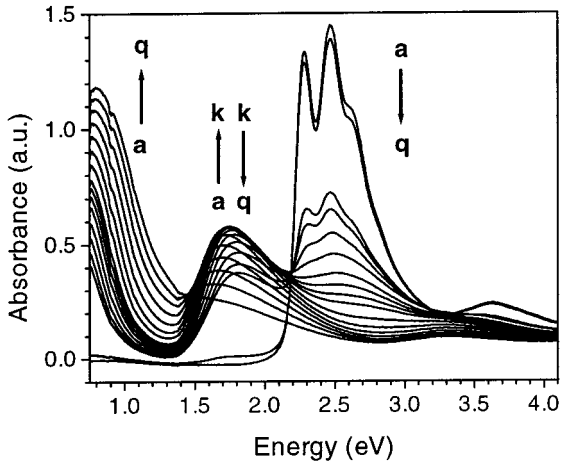

Figure 6. Spectroelectrochemistry of LPEB in 0.1 M $LiClO_4$/acetonitrile as a function of the potential applied vs Fc/Fc^+: (a) −0.15 V, (b) −0.05 V, (c) −0.03 V, (d) −0.02 V, (e) +0.01 V, (f) +0.06 V, (g) +0.11 V, (h) +0.16 V, (i) +0.21 V, (j) +0.26 V, (k) +0.36 V, (l) +0.46 V, (m) +0.56 V, (n) +0.66 V, (o) +0.76 V, (p) +0.86 V, and (q) +0.96 V.

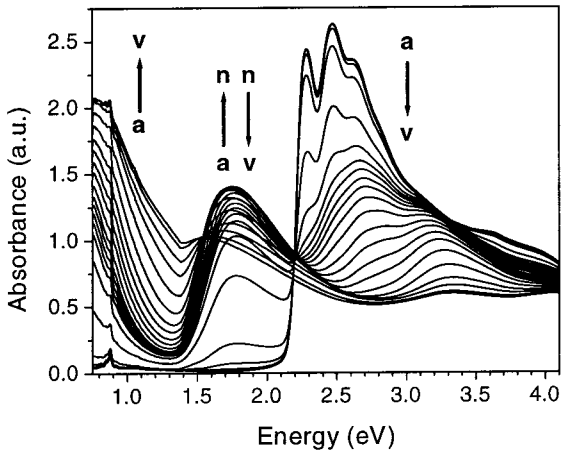

Figure 7. Spectroelectrochemistry of SPEB in 0.1 M $LiClO_4$/acetonitrile as a function of the potential applied vs Fc/Fc^+: (a) −0.15 V, (b) −0.10 V, (c) −0.07 V, (d) −0.05 V, (e) −0.02 V, (f) +0.01 V, (g) +0.03 V, (h) +0.06 V, (i) +0.11 V, (j) +0.16 V, (k) +0.21 V, (l) +0.26 V, (m) +0.36 V, (n) +0.46 V, (o) +0.56 V, (p) +0.66 V, (q) +0.76 V, (r) +0.86 V, (s) +0.96 V, (t) +1.06 V, (u) +1.16 V, and (v) +1.26 V.

Spectroelectrochemical Properties. The spectroelectrochemical properties of LPEB and SPEB were compared by spectroelectrochemistry as shown in Figures 6 and 7, respectively. The observed band gap was found to be 2.15 eV for both polymers, when taken at the onset of the $\pi-\pi^*$ transition. The similar spectroscopic behavior noticed for these two polymers brings out the dominance of the PEB arms in the star. The $\pi-\pi^*$ transition is split as a result of vibronic coupling as noticed in neutral alkylated PEDOT.[5] In both sets of spectra, we observe a very rapid decrease of the $\pi-\pi^*$ transition at −0.04V vs Fc/Fc^+. With increasing potential, two new bands appear with the first in the visible region at about 1.75 eV (708 nm) and the second in the near-infrared at about 0.75 eV (1650 nm) as typically observed with this type of polymer. Importantly in both cases, the band at 1.75 eV stops growing at +0.36 V for LPEB and +0.46 V for SPEB vs Fc/Fc^+. This is attributed to the beginning of band mixing as this process is reversible and well below the potential for overoxidation. Note that the band in the near-infrared increases constantly upon oxidation up to

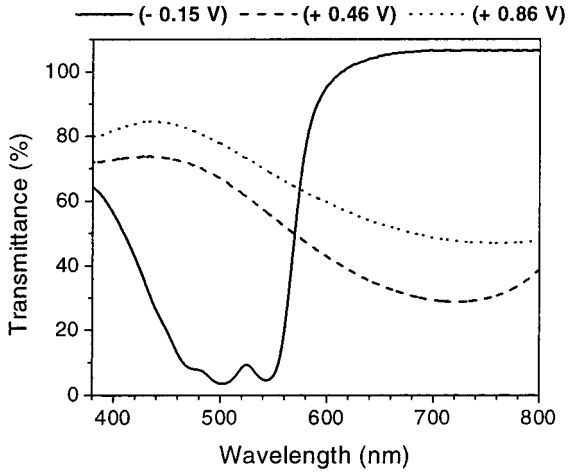

Figure 8. Transmittance of LPEB in the visible region, as a function of wavelength (nm) for three different potentials: −0.15 V (solid), +0.46 V (dash), and +0.86 V (dot) vs Fc/Fc^+.

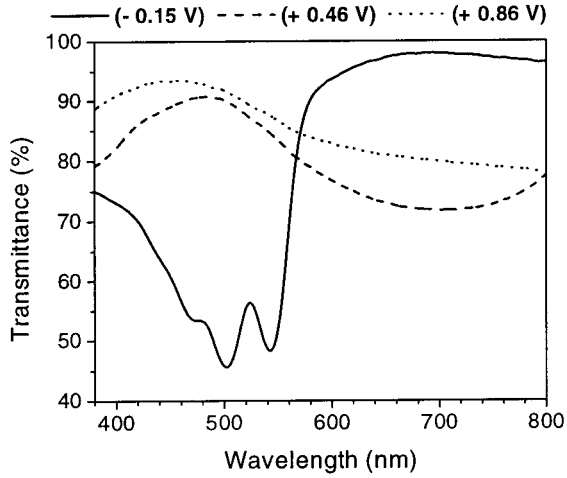

Figure 9. Transmittance of SPEB in the visible region, as a function of wavelength (nm) for three different potentials: −0.15 V (solid), +0.46 V (dash), and +0.86 V (dot) vs Fc/Fc^+.

+1.16 V for SPEB and +0.96 V for LPEB vs Fc/Fc^+. Above these potentials, a subsequent decrease of the near-IR absorption (not shown in the figures) occurs due to full overoxidation of the polymer. It should also be noted that in the doped spectrum of the SPEB the absorbance of the $\pi-\pi^*$ transition cannot decrease as much as the LPEB, because of the absorbance of the PTPA conjugated core at 3.26 eV (380 nm). Comparing the electrochemical and spectroelectrochemical results, it is possible to limit the applied potential to a range where only the PEB arms redox is accessed while still attaining nearly the entire range of the optical change.

To more completely understand the changes occurring in the visible region that are important for consideration as electrochromic materials, Figures 8 and 9 show the film transmittance of LPEB and SPEB at −0.15, +0.46, and +0.86 V vs Fc/Fc^+. In addition, they allow us to determine the wavelength corresponding to the maximum optical contrast which happens to be at 500 nm (2.48 eV) for both polymers. Note that the highest contrast ratio at 500 nm is obtained by oxidizing the polymers at potentials up to at least +0.86 V vs Fc/Fc^+, but little is gained in going beyond potentials of +0.46 V. This effect is more prominent in LPEB where the optical contrast is increased by 14% using the higher

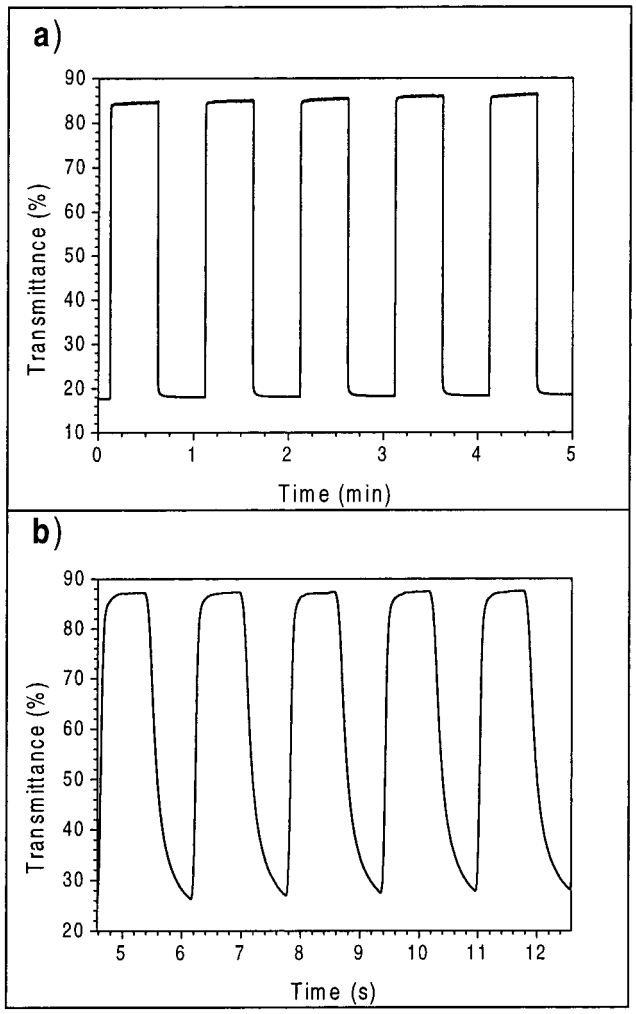

Figure 10. Variation of transmittance for LPEB as a function of time for five switches between −0.25 and +0.86 V vs Fc/Fc^+ in 0.1 M $LiClO_4$/acetonitrile for different step times: (a) 30 s and (b) 1 s.

switching potential, as opposed to SPEB where the difference is only 3%.

Switching Properties. The experiments carried out by spectroelectrochemistry have demonstrated the ability of SPEB and LPEB to switch between its neutral (red) and doped (blue) states with a significant change in transmittance at 500 nm. To investigate the switching time of these polymers and the stability of their electrochromic changes, double potential step switching experiments were conducted between −0.25 and +0.86 V vs Fc/Fc^+. The polymers were switched using different step times (30 and 1 s to allow determination of full switching contrast and switching speeds, respectively) as shown in Figure 10 (LPEB) and Figure 11 (SPEB). Both polymers demonstrated fast switchability since the time to achieve 95% of the maximum optical contrast was less than 0.2 s in both cases. With 30 s steps, the LPEB displayed a contrast ratio of 65−70% while the SPEB**s** contrast was lower at 45% due to the absorbance of the core.

To study long-term switching stability and ensure that a full electrochromic shift had been attained, switching experiments were carried out with steps of 1 s where a contrast ratio $\Delta\%T$ of 43% for SPEB and 65% for LPEB was measured. The polymer films cast on an ITO-covered glass electrode were switched between −0.25 and +0.86 V vs Fc/Fc^+ while monitoring the

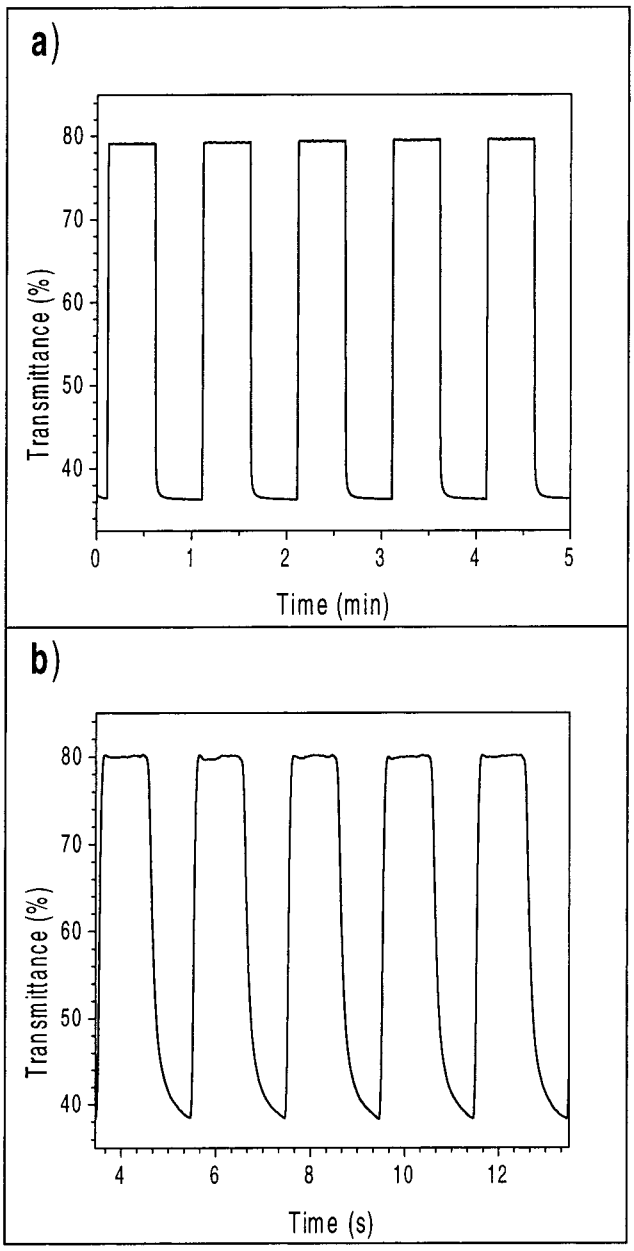

Figure 11. Variation of transmittance for SPEB as a function of time for five switches between −0.25 and +0.86 V vs Fc/Fc$^+$ in 0.1 M $LiClO_4$/acetonitrile for different step times: (a) 30 s and (b) 1 s.

optical contrast ($\Delta\%T$) at 500 nm (Figure 12) and the charge involved in the electrochemical process (Figure 13) as a function of the number of switches. It is noteworthy that the LPEB does not retain its high contrast ratio when switched deeply. A rapid decrease is observed within the first 200 switches, where $\Delta\%T$ drops from 65% to about 46%. Subsequently, a monotonic decrease in $\Delta\%T$ occurs as the contrast ratio is lowered to about 8% after 2500 switches. The SPEB features a different behavior as there is no immediate drop in $\Delta\%T$ during the initial switches, and only a monotonic decrease occurs down to about 16% after 4500 switches. As a consequence, after about 700 switches, SPEB exhibits a higher contrast ratio than LPEB. Moreover, after 2500 switches, SPEB still retains a contrast of about 25% which represents more than the half of its original value.

Figure 13 shows the relative electroactivity of both polymers determined using the ratio (Q/Q_0) representing

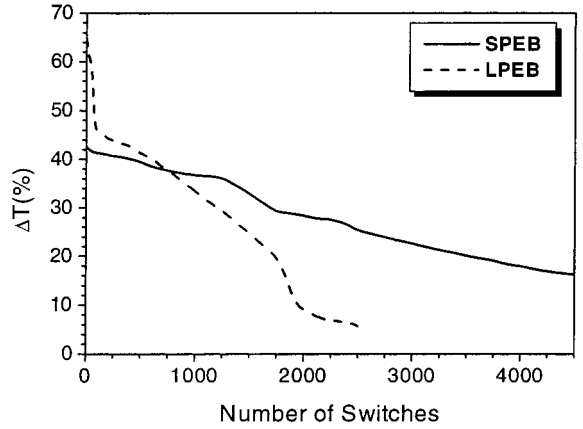

Figure 12. Evolution of the optical contrast for LPEB and SPEB as a function of the number of 1 s switches between −0.25 and +0.86 V vs Fc/Fc$^+$.

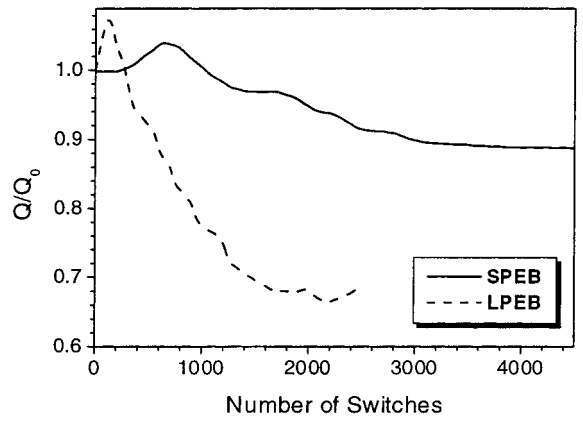

Figure 13. Evolution of the electroactivity for LPEB and SPEB as a function of the number of 1 s switches between −0.25 and +0.86 V vs Fc/Fc$^+$.

the charge involved in the electrochemical process after the *n*th cycle relative to the initial switching charge after break-in of the polymer's redox processes. For LPEB and SPEB, an initial increase of the electroactivity is observed. This phenomenon is not surprising as even after the short break-in period further electroactive sites can be activated in a freshly cast polymer film. For the case of the LPEB, after 200 doping/dedoping cycles a maximum redox efficiency is reached as the number of electroactive sites is optimized. This optimization time is longer for SPEB as it takes about 700 cycles. After reaching a maximum in electroactivity, both LPEB and SPEB lose electroactivity with the LPEB degrading much more rapidly than SPEB. Note that LPEB loses about 30% of its electroactivity after 2000 switches which, compared to most other conducting polymers, is considered a relatively stable switching material. At the same time, SPEB displays a very high retention of 90% of its original electroactivity after 4500 switches. In fact, the electroactivity of SPEB plateaued at about 3000 switches and only decreased very slightly prior to the end of the experiment. The superior electrochemical stability of SPEB observed in this experiment sheds light on the difference in the optical properties seen previously during switching. The electroactivity of a conjugated polymer is found to decrease upon degradation, leading to a lower conjugation length and yielding lower optical contrast. It is likely that SPEB would retain a useful switching stability to greater than 10 000 switches and, in her-

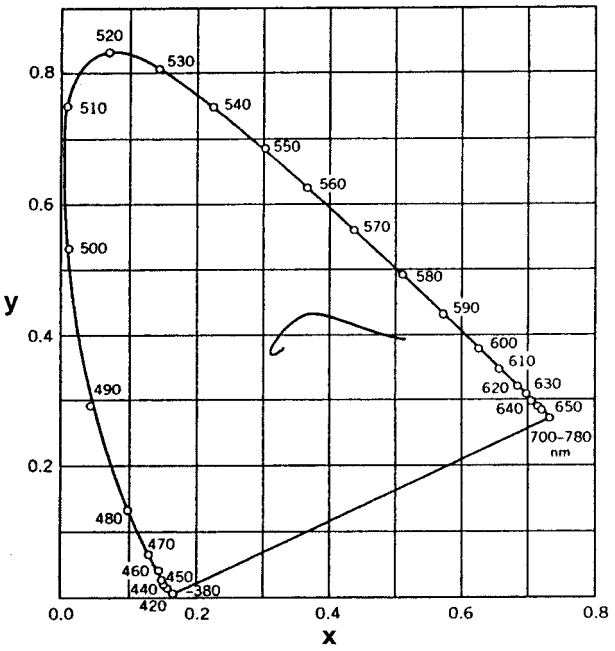

Figure 14. Representation of the color trace of SPEB in the CIE 1931 *xy* chromaticity diagram. The trace starts from the right (red neutral state of the polymer) and terminates at the left (blue doped state) after passing through a green intermediate.

metically sealed devices, would perform extremely well. SPEB exhibits an enhanced solubility relative to LPEB in the casting solution. Comparison of the film quality between the two materials shows SPEB to be more homogeneous and of higher quality overall. In fact, during the thermochromic observations discussed earlier, LPEB films had a tendency to crack upon cooling, while the star polymer films exhibited a higher degree of mechanical integrity. This film quality, while difficult to quantitate, causes SPEB to have a better stability of its optical properties.

Electrochromic Properties. The electrochemical, spectroelectrochemical, and switching results illustrate the usefulness of linear and star PEB for electrochromic applications. If these polymers are to be considered for use in practical electrochromic devices, it is important to develop an understanding of their colors in both doped and undoped states along with the mechanism of color change. For commercial and industrial applications, a precise definition of color is required. Therefore, we studied the two polymers by colorimetry and expressed the results in the CIE 1931 *Yxy* color space as recommended by the "Commission Internationale de l'Eclairage" (CIE).[20] The complete CIE 1931 xy diagram, including the spectral locus, is presented in Figure 14 for SPEB. A close-up of the color traces in the 1931 *xy* chromaticity diagram for LPEB and SPEB is shown in Figure 15. It is important to note the initial and final applied potentials as each polymer was observed to switch from red (neutral) to blue (doped) with an intermediate green state. The color tracks have a very similar shape for both polymers. First, as the potential is increased from the neutral form, the *x* coordinate decreases and the *y* coordinate increases initially and subsequently decreases. This behavior is due to the doping process as the absorbance of the higher energy $\pi-\pi^*$ transition is depleted with the concurrent growth of lower energy charge carrier transitions. As a result, the absorbance maximum is shifted to longer wavelengths, and the complementary color actually seen by the observer shifts to shorter wavelengths. This is evident on the full *xy* chromaticity diagram (Figure 14) as the spectral locus tracks to lower wavelength. Note that the point of maximum *y* value corresponds to the intermediate green state for both LPEB and SPEB. The *Yxy* values for the red, green, and blue states are summarized in Table 2.

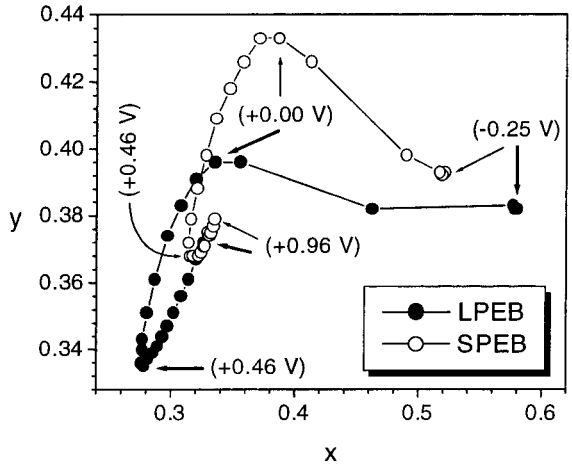

Figure 15. Close-up of the CIE 1931 *xy* chromaticity diagram of LPEB (filled circle) and SPEB (open circle). The potentials are given vs Fc/Fc^+.

Table 2. CIE 1931 *Yxy* Coordinates for SPEB and LPEB

color	SPEB	LPEB
red	$Y = 363$	$Y = 292$
	$x = 0.521$	$x = 0.580$
	$y = 0.393$	$y = 0.382$
green	$Y = 361$	$Y = 138$
	$x = 0.371$	$x = 0.335$
	$y = 0.433$	$y = 0.396$
blue	$Y = 371$	$Y = 191$
	$x = 0.315$	$x = 0.278$
	$y = 0.368$	$y = 0.335$

An interesting feature can be noticed in the *xy* diagrams: both polymers show a sharp tail at high potentials. It is noteworthy that the beginning of the tail is located at the exact same potential where the band mixing was observed in the spectroelectrochemistry. Moreover, this tail also reflects a bleaching at high oxidation potentials as observed for PEDOT and its derivatives.[7] This bleaching was apparent in Figures 8 and 9 as between +0.46 and +0.86 V vs Fc/Fc^+ both polymers exhibited a higher transmittances in the visible region. The luminance, which is the third coordinate in the *Yxy* diagram, represents the brightness of a color and provides information about the transparency of a sample over the entire visible range of light. The relative luminance of LPEB and SPEB is presented in Figure 16 as a function of the applied potential. Note that the minimum in the luminance corresponds to the dark green intermediate state. As expected, the relative luminance of the fully doped state is higher than that of the neutral state due to the depletion of the $\pi-\pi^*$ transition in the visible region. Note that the relative luminance is a more meaningful measurement than the transmittance at a fixed wavelength since it gives information on the entire visible region. It is especially informative for electrochromics because a low value signifies an opaque material, whereas a high value is characteristic of a fully transparent material.

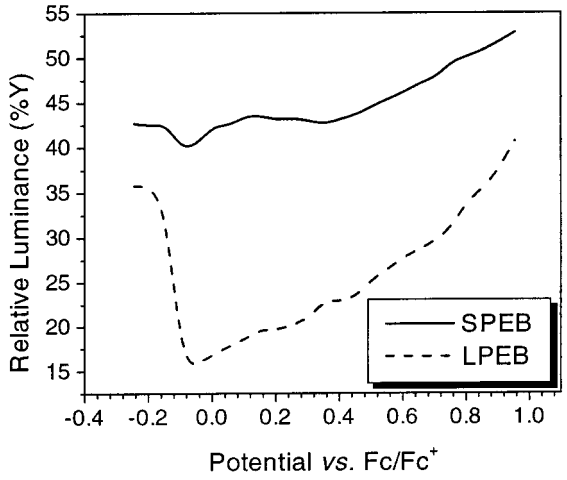

Figure 16. Relative luminance of LPEB and SPEB as calculated from the *Yxy* coordinates as a function of the potential applied vs Fc/Fc^+.

In summary, we have successfully developed a synthetic method for the preparation of poly(3,4-ethylenedioxythiophene−didodecyloxybenzene), in both linear and star structures. The branched star structure was confirmed by SEC characterization. As expected, the introduction of an EDOT moiety along the conjugated backbone resulted in a low half-wave potential leading to a fairly clear separation between the oxidation of the conjugated poly(triphenylamine) core and the electroactivity of the PEB. As such, it is possible to access almost the entire range of optical properties with this new star polymer without oxidizing the core significantly. Both LPEB and SPEB have demonstrated an interesting potential as electrochromic polymers for polymer-based devices as they are able to produce the three basic colors in the RGB system: red, green, and blue. According to spectroelectrochemical, switching, and colorimetry measurements, the presence of the poly(triphenylamine) core improves the stability of the optical properties upon switching and confers a better resistance to overoxidation. As a conclusion, this new star polymer combines the assets of the excellent electrochromic properties of its linear parent with better thermal stability, processability, and durability.

Experimental Section

General. EDOT (Baytron M) was purchased from Bayer AG and distilled before use. All other reagents and solvents were used as purchased from Aldrich Chemical. 1,4-Dibromo-2,5-didodecylbenzene was prepared following a previous reported.[21] Bromothiophene-capped poly(triphenylamine) was prepared as reported before.[10] ^{1}H NMR spectra were recorded on a Hitachi R-1500 FT-NMR spectrometer at 60 MHz. ^{13}C NMR spectra were recorded on a TECMAG QE-300 FT-NMR spectrometer at 75 MHz. Infrared spectra were recorded on a Nicolet 750 FTIR spectrometer. UV−vis spectra were recorded on a HP 8452A UV−vis diode array spectrophotometer. Solid-state UV−vis spectra were obtained by casting a thin film from chloroform solution of the polymers onto quartz substrates. Size exclusion chromatography was conducted on a Hewlett-Packard series 1050 HPLC with a Hewlett-Packard 1047A refractive index detector and a Viscotek T60 light scattering and viscosity detector; data analysis was done using the Viscotek Trisec GPC software version 3.0. One Polymer Laboratories PL gel 5μ mixed-D column was used with THF as solvent. TGA was conducted on a Perkin-Elmer TGA7 thermogravimetric analyzer under nitrogen with a heating rate of 20 °C/min. Elemental analyses were carried out by Schwarzkopf Microanalytical Laboratories, Inc. High-resolution mass spectrometry (HRMS) was carried out by the Spectroscopic Services Laboratory of the University of Florida.

Cyclic voltammetry was carried out with an EG&G Princeton Applied Research model 273 potentiostat/galvanostat employing a platinum button working electrode (diameter 1.6 mm; area 0.02 cm^2), a platimum wire counter electrode, and a silver wire pseudo-reference electrode. The electrolyte used was 0.1 M lithium perchlorate in distilled acetonitrile. Electrolyte solutions were further dried with activated 4 Å molecular sieves. The potential of the pseudo-reference electrode was calibrated versus ferrocene/ferricenium (Fc/Fc^+) in the same electrolyte, as recommended by IUPAC.[22] All potentials are reported versus Fc/Fc^+. The scan rate was set to 20 mV/s for cyclic voltammetry. Corrware II software from Scribner Associates was used for data acquisition and instrument control. Polymer films were cast with a microsyringe on the surface of the working electrode from 2 μL of a 2% solution in chloroform. These films were allowed to dry for 2 h at room temperature prior to characterization in order to evaporate the solvent.

Spectroelectrochemical spectra were recorded on a Varian Cary 5E UV−vis−NIR spectrophotometer at a scan rate of 600 nm/min. A three-electrode cell assembly was used where the working electrode was an ITO-coated glass (7 × 50 × 0.6 mm, 20 Ω/□, Delta Technologies Inc.); the counter was a platinum wire and a silver wire pseudo-reference. The potentials were applied using the same EG&G potentiostat as previously described, and the data were recorded with Corrware II software for electrochemical data and with the a Varian Cary Win-UV for spectral data. The polymer films were also cast with a microsyringe using 20 μL of a 2% solution (covered area: 1.05 cm^2).

Colorimetry measurements were obtained using a Minolta CS-100 chroma meter and CIE recommended normal/normal (0/0) illuminating/viewing geometry for transmittance measurements.[23] A similar three-electrode cell as described for spectroelectrochemistry was employed. The potential was controlled by the same EG&G potentiostat. The sample was illuminated by a D50 (5000 K) back light source in a light booth designed to exclude external light. The color coordinates are expressed in the CIE 1931 *Yxy* color space where the *Y* value is a measure of the luminance in cd/m^2. The relative luminance, expressed in percent, was calculated as the ratio of the *Y* value measured on the sample by the Y_0 value corresponding to an electrolyte/ITO background. Note that relative luminance is reported as opposed to absolute luminance.[24]

2-Trimethyltin−3,4-ethylenedioxythiophene (1). 3,4-Ethylenedioxythiophene (EDOT) (6.39 g, 45 mmol) was dissolved in THF (50 mL), and the solution was cooled to −78 °C. Butyllithium (28.1 mL, 1.6 M in hexane, 45 mmol) was added dropwise, and the mixture was stirred at −78 °C for 1 h. Trimethyltin chloride (45 mL, 1 M in hexane, 45 mmol) was then added dropwise, and the mixture was allowed to warm to ambient temperature with stirring overnight. Water (30 mL) was added followed by ether (50 mL). The phases were separated, and the organic layer was dried ($MgSO_4$) and evaporated to dryness to give the product as a brown solid (10.8 g, 79%). GC/MS: 306 (correct M^+ with Sn isotope pattern). ^{1}H NMR ($CDCl_3$): δ = 6.57 (s, 1H, CH), 4.17 (m, 4H, OCH_2CH_2O), 0.35 (s, 9H, $Sn(CH_3)_3$).

1-(3,4-Ethylenedioxythienyl)-4-bromo-2,5-bis(dodecyloxy)benzene (2). Compound **1** (3.1 g, 10.2 mmol), 1,4-dibromo-2,5-didodecyloxybenzene (10.0 g, 16.6 mmol), and $Pd(PPh_3)_2Cl_2$ (0.29 g, 0.4 mmol) were added to DMF (100 mL), and the mixture was placed under vacuum for 10 min followed by purging with argon for 10 min. The mixture was stirred at 100 °C overnight. The DMF was evaporated, and the last traces of solvent were removed by coevaporation with methanol. Hexane (150 mL) was added and the mixture was filtered. The solvent was evaporated to give a pale yellow solid. The residue was purified by column chromatography (eluent hexane/ethyl acetate (0−2%)) followed by recrystallization from pentane to give the product as a yellow solid (4.1 g, 61%); mp 62−64 °C. ^{1}H NMR ($CDCl_3$): δ = 7.64 (s, 1H, CH), 7.10 (s, 1H, CH), 6.38 (s, 1H, thiophene CH), 4.26 (m, 4H, OCH_2CH_2O), 3.99 (4H, m, 2 × OCH_2), 1.27 (m, 44H, 22 × CH_2), 0.88 (m,

6H, 2 × CH_3). ^{13}C NMR ($CDCl_3$): δ = 14.06, 22.66, 25.69, 28.78, 29.12, 29.30, 29.32, 29.59, 29.62, 29.82, 31.90, 62.06, 62.72, 67.25, 69.57, 95.56, 109.12, 112.32, 116.54, 118.76, 121.03, 145.16, 151.73, 151.83, 155.24. HRMS $C_{36}H_{57}BrO_4S$: calcd, 665.8031; obsd, 665.8037.

1-(2-Bromo-3,4-ethylenedioxythiophene)−4-bromo-2,5-didodecyloxybenzene (3). EDOT derivative **2** (0.5 g, 0.75 mmol) was dissolved in chloroform, and NBS (0.14 g, 0.79 mmol) was added in six portions over 10 min. The mixture was stirred at ambient temperature for 2 h. The solvent was then removed under reduced pressure, and the crude residue was purified by column chromatography (neutral alumina, eluent hexane/ethyl acetate (0−2%)) as a white solid (0.45 g, 80%). The absence of the thiophene proton (previously at δ = 6.4 ppm) in **2** could be clearly seen in the ^1H NMR spectrum of the product. ^1H NMR ($CDCl_3$): δ = 7.67 (1H, s, ArH), 7.09 (1H, s, ArH), 4.31 (4H, m, EDOT OCH_2), 4.00 (4H, m, benzene-OCH_2), 1.28 (40H, m, 20 × CH_2), 0.89 (6H, m, 2 × CH_3).^{13}C NMR ($CDCl_3$): δ = 14.06, 22.66, 25.69, 28.78, 29.12, 29.30, 29.32, 29.59, 29.62, 29.82, 31.90, 60.39, 61.28, 67.25, 69.57, 81.71, 107.96, 113.11, 116.54, 119.68, 120.75, 151.21, 152.51, 152.76, 158.64. HRMS $C_{36}H_{56}Br_2O_4S$: calcd, 744.6992; obsd, 744.7010.

Linear Poly(3,4-ethylenedioxythiophene)−2,5-didodecyloxybenzene) (LPEB). The dibromo compound **3** (0.51 g, 0.69 mmol) was dissolved in THF (10 mL) and CH_3MgBr (0.55 mL, 1.4 M in toluene/THF, 0.72 mmol) added dropwise, and the mixture was heated to reflux for 3 h. Ni(dppp)Cl_2 (4 mg, 7.38 mmol) was then added and the mixture refluxed overnight. The solution was allowed to cool to ambient temperature and then poured into methanol to give a bright red solid. The solid was collected by filtration and Soxhlet extracted with MeOH, then hexanes, and finally chloroform. The chloroform was evaporated to give the polymer LPEB as a bright red solid (90 mg, 22%). ^1H NMR ($CDCl_3$): δ = 7.65 (s, 2H, CH), 4.35 (m, 4H, OCH_2CH_2O), 4.06 (4H, m, 2 × OCH_2), 1.25 (m, 44H, 22 × CH_2), 0.87 (m, 6H, 2 × CH_3). Anal. Calcd for $C_{36}H_{56}O_4S$: C, 73.94; H, 9.65; S, 5.48. Obsd: C, 71.95; H, 9.23; S, 6.12.

Star Poly(3,4-ethylenedioxythiophene)−2,5-didodecyloxybenzene) (SPEB). The dibromo compound **3** (0.9 g, 1.21 mmol) was dissolved in THF, and MeMgBr (0.9 mL, 1.4 M in toluene/THF, 1.26 mmol) was added dropwise. The mixture was refluxed for 3 h. The mixture was allowed to cool to ambient temperature and was then added dropwise over 2 h to a refluxing solution of bromothiophene-capped poly(triphenylamine) **10** (0.05 g, 0.12 mmol) and Ni(dppp)Cl_2 (10 mg, 18.45 mmol) in THF. The mixture was refluxed overnight. After cooling to ambient temperature, the solution was poured into MeOH to produce a bright red precipitate. The solid was collected by filtration and Soxhlet extracted with MeOH, then hexanes, and finally chloroform. The chloroform was evaporated to give the polymer (SPEB) as a bright red solid (420 mg, 62%). ^1H NMR ($CDCl_3$): δ = 7.65 (s, 2H, CH), 7.3−7.8 (br PTPA core), 4.35 (m, 4H, OCH_2CH_2O), 4.06 (4H, m, 2 × OCH_2), 1.25 (m, 44H, 22 × CH_2), 0.87 (m, 6H, 2 × CH_3). Anal. Calcd for $(C_{22}H_{14}NS)(C_{36}H_{56}O_4S)_{10}$: C, 74.32; H, 9.38; S, 5.71. Obsd: C, 70.15; H, 8.55; S, 6.07.

Acknowledgment. Funding of this work by the U.S. Air Force (AFRL/MLBP F33615-97-C-5090 along with AFOSR F49620-97-1-0232 and F49620-96-1-0067) is gratefully acknowledged. The authors also acknowledge the NSF REU Site at the University of Florida and Scribner Associates for providing Corrware II Software.

References and Notes

(1) Skotheim, T. A.; Elsenbaumer, R. L.; Reynolds, J. R. *Handbook of Conducting Polymers*, 2nd ed.; Marcel Dekker: NewYork, 1998.
(2) Dietrich, M.; Heinze, J.; Heywang, G.; Jonas, F. *J. Electroanal. Chem.* **1994**, *369*, 87.
(3) Heywang, G.; Jonas, F. *Adv. Mater.* **1992**, *4*, 116.
(4) Pei, Q.; Zuccarello, G.; Ahlskog, M.; Inganas, O. *Polymer* **1994**, *35*, 1347.
(5) Sankaran, B.; Reynolds, J. R. *Macromolecules* **1997**, *30*, 2582.
(6) Sapp, S. A.; Sotzing, G. A.; Reynolds, J. R. *Chem. Mater.* **1998**, *10*, 2101.
(7) Kumar, A.; Welsh, D. M.; Morvant, M. C.; Piroux, F.; Abboud, K. A.; Reynolds, J. R. *Chem. Mater.* **1998**, *10*, 896.
(8) Roovers, J. *Trends Polym. Sci.* **1994**, *2*, 294.
(9) Wang, F.; Rauh, R. D.; Rose, T. L. *J. Am. Chem. Soc.* **1997**, *119*, 11106.
(10) Wang, F.; Wilson, M. S.; Rauh, R. D.; Schottland, P.; Reynolds, J. R. *Macromolecules* **1999**, *32*, 4272.
(11) Irvin, J. A.; Reynolds J. R. *Polymer* **1998**, *39*, 2339.
(12) Loewe, R. S.; Khersonsky, S. M.; McCullough, R. D. *Adv. Mater.* **1999**, *11*, 250.
(13) See Figure 12 in: Roovers, J.; Zhou, L.; Toporowski, P. M.; Zwan, M.; Iatrou, H.; Hadjichristidis, N. *Macromolecules* **1993**, *26*, 4324.
(14) DiCésare, N.; Belletête, M.; Leclerc, M.; Durocher, G. *Chem. Phys. Lett.* **1998**, *291*, 487.
(15) Leclerc, M.; Faïd, K. *Adv. Mater.* **1997**, *9*, 1087.
(16) DiCésare, N.; Belletête, M.; Durocher, G.; Leclerc, M. *Chem. Phys. Lett.* **1997**, *275*, 533.
(17) Hanna, R.; Leclerc, M. *Chem. Mater.* **1996**, *8*, 1512.
(18) Leclerc, M.; Fréchette, M.; Bergeron, J.-Y.; Ranger, M.; Lévesque, I.; Faïd, K. *Macromol. Chem. Phys.* **1996**, *197*, 2077.
(19) McCullough, R. D.; Tristram-Nagle, S.; Williams, S. P.; Lowe, R. D.; Jayaraman, M. *J. Am. Chem. Soc.* **1993**, *115*, 4910.
(20) CIE: Colorimetry (Official Recommendations of the International Commision on Illumination), CIE Publication No. 15, Paris, 1971.
(21) Ruiz, J. P.; Dharia, J. R.; Reynolds, J. R.; Buckley, L. J. *Macromolecules* **1992**, *25*, 849.
(22) Gritzner, G.; Kuta, G. *J. Pure Appl. Chem.* **1984**, *56*, 461.
(23) Nassau, K. *Color for Science, Art and Technology*; Elsevier: Amsterdam, 1998.
(24) Overheim, R. D.; Wagner, D. L. *Light and Color*; Wiley: New York, 1982; p 77.

MA9918506